Long-term influence of high alkalinity on the performance of photosynthetic biogas upgrading

María del Rosario Rodero[a,b], Cristian Alfredo Severi[a,b], Ricardo Rocher-Rivas[a,c], Guillermo Quijano[c], Raúl Muñoz[a,b]*

[a] Department of Chemical Engineering and Environmental Technology, University of Valladolid, Dr. Mergelina s/n., 47011, Valladolid, Spain.

[b] Institute of Sustainable Processes, University of Valladolid, 47011, Valladolid, Spain.

[c] Laboratory for Research on Advanced Processes for Water Treatment, Instituto de Ingeniería, Unidad Académica Juriquilla, Universidad Nacional Autónoma de México, Blvd. Juriquilla 3001, Querétaro 76230, México.

*corresponding author: mutora@iq.uva.es

ABSTRACT

The alkalinity of the cultivation medium plays a key role on photosynthetic biogas upgrading, exerting impact not only on the mass-transfer of CO_2 and H_2S in the biogas scrubbing column but also on the subsequent CO_2 uptake or stripping to the atmosphere. The long-term performance of algal-bacterial processes devoted to the concomitant removal of CO_2 and H_2S from biogas in a 180 L open pond interconnected to a 2.5 L biogas scrubbing column via an external liquid recirculation of supernatant from a 8 L conical settler under process operation at high inorganic carbon (IC) concentrations was assessed. The influence of biomass concentration in the cultivation medium on process performance was also evaluated. CO_2 concentrations in the upgraded biogas fluctuated between 1.5 and 4.4% at IC concentrations in the cultivation medium of 1200 mg C L^{-1}, and remained almost constant (0.7 ± 0.1%) at

IC concentrations > 2400 mg C L^{-1}. However, the increase in the IC concentration from 1203 to 3476 mg C L^{-1} entailed an increase in C-CO_2 stripping from 14.5 to 33.4% of the IC input to the system. The increase in biomass concentration from 0.33 to 1.38 g SSV L^{-1} entailed a reduction in CO_2 removal of 1.1% even under process operation at high alkalinity. H_2S removal efficiencies of 100% were achieved regardless the IC or biomass concentration.

Keywords: algal-bacterial symbiosis; alkalinity; biomass concentration; biogas upgrading; biomethane.

1. Introduction

Biogas constitutes the most valuable byproduct from the anaerobic degradation of residual organic substrates. Typically, biogas consists of CH_4 (40-75%), CO_2 (25-50%), H_2S (0.005-3%) and other components such as O_2, N_2, NH_3, siloxanes, halogenated hydrocarbons and water at trace level concentrations [1]. The energy potential of biogas, due to its high CH_4 content, has promoted the use of this bioenergy source as a substitute of fossils fuels [2]. In this context, the global production of biogas has increased from 0.28 to 1.31 exajoule during the period 2000-2016, which represented a total volume of biogas of approx. 60.8 billion Nm^3 [3]. However, the presence of pollutants, such as CO_2 and H_2S, prevents the direct use of biogas as a vehicle fuel or its addition into natural gas networks, which requires concentrations of CH_4 > 90%, CO_2 < 2–4%, O_2 < 0.001–1% and H_2S + COS < 5 mg/Nm^3 according to most international regulations [4,5]. CO_2 removal increases the specific biogas energy content, reduces its transportation costs and results in lower greenhouse gas emissions during biogas combustion, while the removal of H_2S is crucial due to its hazardous, malodorous and corrosive nature [6,7].

Physical-chemical technologies including water/organic/chemical scrubbing, pressure swing adsorption and membrane separation for CO_2 removal, and *in situ* precipitation, adsorption on activated carbon or metal ions, absorption and membrane separation for H_2S removal are widely applied for biogas upgrading [8]. Nevertheless, most of these technologies are not able to support the simultaneous removal of both components and typically entail a high energy and chemical consumption, which limit the environmental and economic sustainability of biomethane [9]. Likewise, biological technologies (i.e. biological methanation of CO_2 with H_2 and biofiltration or *in situ* microaerobic digestion for H_2S removal) must be combined to remove CO_2 and H_2S from biogas [10]. In this context, biogas upgrading based on algal–bacterial symbiosis is a cost-competitive alternative for the concomitant removal of H_2S and CO_2 from biogas in an environmentally sustainable way [11]. This platform technology is based on the light-driven CO_2 uptake by microalgae and the oxidation of H_2S to S^0/SO_4^{2-} by sulfur-oxidizing bacteria promoted by the oxygen photosynthetically generated [12]. In addition, the liquid fraction of digestates from anaerobic digestion can be used as a free water and nutrient source to support algal-bacterial growth, which represents an economic and environmental benefit of this technology compared to its physical/chemical and biological counterparts [13].

Recent works have evaluated the influence of operational and environmental parameters such as the wavelength, intensity and photoperiod of the light source [14–16], alkalinity and temperature of the cultivation broth [17], the diffuser type [18], liquid to biogas (L/G) ratio and gas-liquid flow configuration in the scrubbing column [19] on the quality of the biogas upgraded. These previous optimizations of the operational parameters allowed to obtain a

biomethane complying with most international standards for its injection into natural gas networks. For instance, Franco-Morgado et al. [20] reported an average biomethane composition of 99.1% CH_4, 0.5% CO_2, 0.6% N_2 and 0.1% O_2 during the integral photosynthetic biogas upgrading in an analogous experimental set-up under indoors conditions. In addition, Marín et al. [21] obtained a CH_4 concentration between 85 and 98% in a pilot experimental set-up over one year operation under outdoor conditions. Rodero et al. [22] designed a control strategy based on the regulation of L/G ratio in order to maintain biomethane quality regardless of environmental fluctuations. In this study, a decrease in the pH of the cultivation medium mediated high liquid flowrates, with the subsequent increase in O_2 stripping and energy demand. In this context, Rodero et al. [17] reported an enhancement on CH_4 content in the upgraded biomethane from 79 to 98% with an increase on the inorganic carbon (IC) concentration in the cultivation medium from 100 to 1500 mg IC L^{-1}. Thereby, an optimum alkalinity capable of maintaining a high pH in the absorption column can support consistent CO_2 and H_2S removals. However, high IC concentrations in the pond could negatively impact on microalgae and bacterial activity due to a detrimental salinity effect, and increase CO_2 stripping from the cultivation medium to the atmosphere, thus limiting the environmental sustainability of photosynthetic biogas upgrading. For instance, de Farias Silva et al. [23] observed that the growth of *Synechococcoccus* PCC 7002 was inhibited at sodium bicarbonate concentrations above 22 g L^{-1} (~3140 mg IC L^{-1}) while Li et al. [24] reported a cell growth decrease from 120 to 1920 mg IC L^{-1} by addition of $NaHCO_3$ in *Chlorella vulgaris*. Besides, an inorganic salt content above 1-2 wt% might cause no salt-tolerant bacteria death due to cell plasmolysis [25]. Likewise, biomass concentration in the cultivation medium could potentially impact on both the CO_2 removal from biogas in the bubble column by promoting the accumulation of large algal-bacterial flocs in the vicinity

of the biogas sparger, which could trigger biogas bubble coalescence and result in an inefficient CO_2 gas-liquid mass transfer [26], and its subsequent photosynthetic assimilation due to light limitation as a result of high biomass cell density.

This study systematically assessed the impact of long-term process operation under high IC concentration in the cultivation medium on the H_2S and CO_2 removal efficiency and robustness during photosynthetic biogas upgrading. Moreover, the influence of the biomass concentration on the performance of the upgrading process was also investigated. Finally, CO_2 stripping from the open pond was determined in order to evaluate the environmental performance of this technology.

2. Materials and methods

2.1. Experimental set-up

The experimental set-up, located indoors at the Institute of Sustainable Processes of Valladolid University (Spain), consisted of a High Rate Algal Pond (180 L) interconnected to a conical settler (8 L) whose supernatant was used as scrubbing solution in a 2.5 L absorption column and returned to the pond (Fig. 1). The pond (length: 202 cm , width: 63 cm, depth: 15 cm) was agitated by a 6-blade paddlewheel at a liquid recirculation velocity of ~20 cm s^{-1}, and illuminated continuously at 1240 ± 512 μmol m^{-2} s^{-1} (measured in different points along the total surface of the pond) by six Phillips LED PCBs (Spain). The pond (1.2 m^2 of illuminated surface) was continuously fed at an inlet flowrate of 3.2 L d^{-1} with a mineral salt medium (MSM) containing (g L^{-1}): 0.58 K_2HPO_4, 1.91 NH_4Cl, 0.10 $MgSO_4 \cdot 7H_2O$, 0.02 $CaCl_2 \cdot 2H_2O$, 5 mL of a trace metal solution (based on the *Spirulina* mineral salt medium [27]) and a mixture of $NaHCO_3$ and Na_2CO_3 according to the IC concentration set in during

each operational stage at a pH of ~10. Synthetic biogas (70% CH_4, 29.5% CO_2 and 0.5% H_2S, Abello Linde (Spain)) was sparged into the scrubbing column (Ø: 4.4 cm, height: 165 cm) using a 2 µm metallic biogas diffuser at a flow rate of 50 ml min^{-1} and a recycling liquid to biogas ratio (L/G) of 0.5 according to Toledo-Cervantes et al. [28]. Despite counter-current flow operation involves higher CO_2 mass transfer rates, co-current mode was selected in this study since it entails lower O_2 and N_2 stripping which results in a higher biomethane quality. In addition, counter-current flow operation results in low dissolved O_2 concentrations in the liquid medium in the vicinity of the biogas sparger (at the bottom of the column), which induces the accumulation of elemental sulphur in the sparger and ultimately hinders CO_2 absorption [28]. Tap water was continuously added to compensate evaporation losses from the open cultivation broth under operation with a zero effluent strategy.

<Fig. 1>

2.2. Operational conditions and sampling procedures

The pond was initially inoculated with a microalgal-bacterial consortium (previously acclimated to the MSM at 1200 mg IC L^{-1}) from an outdoors pond upgrading biogas at the Institute of Sustainable Processes. Three operational strategies were implemented to evaluate the influence of process operation under high alkalinity and biomass concentration in the pond (determined as volatile suspended solids, VSS) on the photosynthetic biogas upgrading efficiency and robustness (Table 1). During stage A, the pond was fed with MSM at an IC concentration of 1200 mg C L^{-1} and operated at a fixed biomass productivity of 15 g VSS m^{-2} d^{-1} set according to the nutrients fed to the pond and considering a phosphorous and nitrogen content in the microalgal biomass of 1 and 8%, respectively [19]. The algal-bacterial biomass was harvested in an external tank via coagulation-flocculation with a synthetic polymeric

flocculant derived from acrylamide (Chemifloc CV-300, Chemipol S.A.) followed by a sedimentation step. During stage B, the IC concentration of the MSM was increased to 2400 mg C L^{-1} and the IC concentration in the pond was adjusted accordingly by addition of $NaHCO_3/Na_2CO_3$ at the beginning of this operational stage. Biomass productivity at 15 g VSS m^{-2} d^{-1} was also maintained during stage B via coagulation-flocculation and sedimentation. In stage C, the operational conditions were similar to those in stage B but no algal-bacterial biomass was harvested.

<Table 1>

Temperature, pH and dissolved oxygen (DO) concentration in the cultivation medium were daily monitored. The photosynthetic active radiation (PAR) was measured at the pond surface at the beginning of the study. Gas samples of 100 μL from the raw biogas and biomethane were drawn twice per week using gas tight syringes to determine the CH_4, CO_2, H_2S, O_2 and N_2 concentrations by GC-TCD. Biogas flowrates at the inlet and outlet of the scrubbing column were also measured to calculate CO_2 and H_2S removal efficiencies. Liquid samples of 100 mL from the MSM and the cultivation medium were drawn twice per week and filtered through 0.20 μm nylon filters to monitor dissolved TN, $N\text{-}NH_4^+$, $N\text{-}NO_2^-$, $N\text{-}NO_3^-$ and IC. Aliquots of 50 mL were also drawn from the cultivation medium twice per week to monitor the VSS concentration. The flowrate of tap water was measured twice per week to determine evaporation losses. The maximum quantum yield of photosystem II (PSII) defined as the ratio of variable to maximal fluorescence (Fv/Fm) was measured at the end of stage C.

2.3. Determination of the mass transfer performance and CO_2 stripping rate

168 The gas-liquid mass transfer performance of the pond was assessed by means of respirometric
169 measurements under controlled conditions, considering the O_2 transfer rate (OTR), O_2
170 production rate (OPR) and the O_2 uptake rate (OUR) according to the following mass balance
171 under light conditions:

172 $$\frac{dC_L}{dt}(gO_2\ m^{-3}h^{-1}) = OTR(gO_2\ m^{-3}h^{-1}) + OPR(gO_2\ m^{-3}h^{-1}) - OUR(gO_2\ m^{-3}h^{-1}) \quad (1)$$

173 Defining the terms OTR, OPR and OUR, Equation 1 can be written as follows:

174 $$\frac{dC_L}{dt}(gO_2\ m^{-3}h^{-1}) = k_L a_{O2}(h^{-1}) \cdot (C^* - C_L)(gO_2\ m^{-3}) + PO_2(gO_2\ gSSV^{-1}h^{-1}) \cdot$$

175 $$X(gSSV\ m^{-3}) - (R_{end} + R_{ex})(gO_2\ m^{-3}h^{-1}) \qquad (2)$$

176 where k_La_{O2}, C^* and C_L are the volumetric oxygen mass transfer coefficient, the O_2 saturation
177 concentration and the O_2 concentration at time *t* in the cultivation medium, respectively. PO_2
178 and X stand for the specific O_2 production and the biomass concentration, respectively. R_{end}
179 and R_{ex} are the volumetric O_2 consumption rates due to endogenous biomass respiration and
180 H_2S oxidation, respectively.

181 In the absence of air-liquid mass transfer and H_2S supply under illuminated conditions,
182 Equation 2 can be written as follows:

183 $$\frac{dC_L}{dt}(gO_2\ m^{-3}h^{-1}) = PO_2(gO_2\ gSSV^{-1}h^{-1}) \cdot X(gSSV\ m^{-3}) - R_{end}(gO_2\ m^{-3}h^{-1}) \quad (3)$$

184 On the other hand, in the absence of air-liquid mass transfer and H_2S supply under dark
185 conditions, Equation 2 can be written as follows:

186 $$\frac{dC_L}{dt}(gO_2\ m^{-3}h^{-1}) = -R_{end}(gO_2\ m^{-3}h^{-1}) = -QO_2(gO_2\ gSSV^{-1}h^{-1}) \cdot X(gSSV\ m^{-3})$$

187 (4)

188 where, QO_2 is the specific O_2 uptake rate.

189 The term R_{ex} can be estimated from the H_2S elimination capacity (EC) and the stoichiometric
190 amount of O_2 required for the full oxidation of the absorbed H_2S into sulfate (1.9 g O_2 g
191 $H_2S_{removed}^{-1}$):

192 $$R_{ex}(gO_2\ m^{-3}h^{-1}) = EC(gH_2S\ m^{-3}h^{-1})\frac{1.9gO_2}{gH_2S} \quad (5)$$

193 The experimental determination of QO_2 and PO_2 required to assess OUR and OPR,
194 respectively, was carried out as follows: when the pond coupled with the biogas scrubbing
195 column reached a stable H_2S removal, an aliquot from the cultivation medium of known
196 biomass concentration was introduced into a 2.1 L glass bottle covered with aluminum foil
197 to avoid photosynthetic activity and the temperature maintained by a water jacket at 28 ±
198 2°C. The test bottle was provided with magnetic stirring (300 rpm) and an optical dissolved
199 O_2 sensor (Vernier, Oregon, USA) connected to a computer for data acquisition each 10 s.
200 No headspace was allowed to avoid interfacial air-liquid mass transfer. Under these
201 conditions, QO_2 was experimentally determined according to Equation 4 (QO_2 being the
202 slope of the C_L vs time plot). The same experimental setup was used for PO_2 determination
203 according to Equation 3, with PO_2 as the fitting parameter. However, in this case the bottle
204 was not covered with aluminum foil and provided with a similar PAR than that of the pond.
205
206 Once OPR and OUR were determined, dark conditions were applied to the pond coupled
207 with the scrubbing column operating under steady conditions by turning off the LED lamps.
208 The optical dissolved O_2 sensor placed in the pond measured the progressive depletion of O_2
209 under dark conditions. When dissolved O_2 concentration reached a minimum value of ~1 g
210 m^{-3}, the LED lamps were turned on. Equation 2 was used to model dissolved O_2 data under
211 illuminated conditions with k_La_{O2} as the fitting parameter. The volumetric CO_2 mass transfer

coefficient (k_La_{CO2}) was then estimated from k_La_{O2} according to Estrada et al.[29]. In brief, the mass transfer coefficient through an aqueous layer for a given gas substrate can be predicted based on its molecular volume at the boiling point (V_m) as:

$$k_L a \; \alpha \; \left(\frac{1}{V_m}\right)^{0.4} \quad (6)$$

Therefore, the mass transfer coefficient k_La_{CO2} can be estimated from a reference coefficient (k_La_{O2}) previously determined in the same reactor under identical operating conditions as follows:

$$\frac{k_L a_{CO2}}{k_L a_{O2}} = \frac{\left(\frac{1}{V_{m,CO2}}\right)^{0.4}}{\left(\frac{1}{V_{m,O2}}\right)^{0.4}} \quad (7)$$

V_m values of 34.0 and 25.6 mL mol^{-1} for CO_2 and O_2 were used [30]. A 4th-order Runge–Kutta method was used to solve Equations 2-4, while the Levenberg–Marquardt method was used for parameter fitting using ModelMaker^{TM} (Cherwell Scientific, UK).

2.4. Analytical methods

The pH was monitored using a pH meter Eutech Cyberscan pH 510 (Eutech instruments, The Netherlands), while an Oxi 330i oximeter (WTW, Germany) was used for DO and temperature determination in the cultivation medium of the pond. CO_2, H_2S, O_2, N_2 and CH_4 biogas and biomethane concentrations were determined using a Bruker 430 GC-TCD (Palo Alto, USA) equipped with the following columns: a CP-Pora BOND Q (25 m × 0.53 mm × 15 μm) and a CP-Molsieve 5A (15 m × 0.53 mm × 15 μm), with helium as the carrier gas at 18 psi. The detector, injector and oven temperatures were maintained at 200, 150 and 45 ºC, respectively. Dissolved IC and TN concentrations were measured by means of a Shimadzu TOC-VCSH analyzer (Japan) equipped with a TNM-1 module. N-NO_3^- and N-

234 NO_2^- concentrations were determined by HPLC-IC according to Serejo et al. [19]. $N\text{-}NH_4^+$
235 concentration was measured using a selective electrode Orion Dual Star (Thermo Scientific,
236 The Netherlands) and VSS analyses were carried out according to standard methods [31].
237 PAR was determined with a LI-250A lightmeter (LI-COR, Germany). The maximum
238 quantum yield of PSII was analyzed using an Aquapen-C fluorometer (Photon Systems
239 Instruments, Czech Republic).
240
241 **3. Results and discussion**
242 **3.1. Photobioreactor performance**
243 The temperature of the cultivation medium in the pond remained almost constant at an
244 average value of 28.2 ± 1.3 ºC, which resulted in an average evaporation rate of 6.9 ± 0.7 L
245 m^{-2} d^{-1} along the three operational stages (Table 2). These water losses by evaporation were
246 similar to those reported by Posadas et al. [32] in a similar outdoor pond during summer
247 conditions. Similar pH values (9.7 ± 0.1) were observed in the three operational stages,
248 supported by the high IC concentrations, which entailed a high buffer capacity of the
249 cultivation medium [15]. On the other hand, the gradual increase in IC concentration exerted
250 a negative impact on microalgal photosynthetic activity, as indicated by the gradual decrease
251 in DO concentration in the cultivation medium. Average DO concentrations of 12.8 ± 1.9,
252 8.6 ± 0.9 and 4.4 ± 1.2 were measured during stages A, B and C, respectively (Table 2). The
253 decrease in DO from stage A to B could be caused by oxidative stress in the
254 cyanobacterial/microalgal culture induced by the increase of the salt content in the pond,
255 which ultimately decreased photosynthetic activity [33]. During stage C, the decrease in DO
256 concentration could be attributed to the lower photosynthetic activity as a result of the higher
257 oxidative stress due to IC accumulation, and consequently, higher salinity in the pond, along

with the lower light availability and the higher endogenous oxygen consumption by photorespiration at the higher biomass concentrations prevailing in stage C. In addition, the maximum photochemical quantum yield (Fv/Fm), which is an indicator of the photosynthetic performance of PSII since it determines the maximal conversion of light into chemical energy of PSII, was 0.28 at the end of the stage C. This value was lower than those typically reported for microalgae and cyanobacteria under no stress conditions (0.46-0.75) [34–36]. Low Fv/Fm indicates an impairment of PSII activity, which may be caused by the inhibition of the activity of the PSII reaction centers or the electron transport at both sides of PSII (donor and acceptor) under stress conditions [37]. Despite the low DO levels recorded in the cultivation medium during stage C, those values were high enough (>2 mg O_2 L^{-1}) to support the aerobic bacterial activity responsible of nitrification and H_2S oxidation to SO_4^{2-} [38,39].

<Table 2>

The initial concentration of VSS in the pond was 1.3 g L^{-1}, which decreased to steady state values of 0.8 ± 0.1 g L^{-1} during stage A (Fig. 2). The increase in the IC concentration during stage B led to a decrease in biomass concentration to steady state concentrations of 0.4 ± 0.1 g VSS L^{-1} (Fig. 2). VSS concentrations during stages A and B were determined by the biomass productivity actively maintained (15 g m^{-2} d^{-1}) and microalgal activity, which itself was influenced by the alkalinity in the pond. During stage C, no biomass was harvested, thus resulting in an increase in biomass concentration up to 1.38 g VSS L^{-1} by the end of stage C. However, biomass productivities (calculated as the increase of the mass of algal-bacterial biomass during a period of time and divided by the illuminated surface) of 13.3 g m^{-2} d^{-1} from day 114 to 126, and 3.4 g m^{-2} d^{-1} from day 126 onwards, were obtained during stage C, which represented a decrease in productivity compared to stages A and B (15 g m^{-2} d^{-1}). The lower

biomass productivity by the end of stage C could be attributed to a higher oxidative stress of microalgae (mediated by the higher alkalinity), a decrease in light availability induced by the higher biomass concentration or the accumulation of inhibitory compounds in the cultivation medium under process operation without effluent and no biomass harvesting.

<Fig. 2>

IC concentration in the cultivation medium of the pond was adjusted at 1200 and 2400 mg C L^{-1} at the beginning of stages A and B, respectively. In stage A, the IC concentration in the pond remained almost constant at 1203 ± 93 mg C L^{-1}. However, the IC concentration in the cultivation medium increased during stages B and C along with the decrease in photosynthetic activity and triggered by the higher IC load in the MSM fed to the pond, reaching values of 3152 and 3814 mg C L^{-1} at the end of stages B and C, respectively (Fig. 2). In this context, Marín et al. [21] reported an increase in IC concentration up to 4138 mg L^{-1} using high-strength digestate (2000 mg IC L^{-1}) in a similar system located outdoors and operated with a zero effluent strategy. In addition, the high pH in the cultivation broth (9.7 ± 0.1) prevented a massive IC loss by CO_2 stripping as latter described in section 3.3.

Similar average TN concentrations in the pond were recorded under steady state in the three stages (609.1 ± 9.7, 558.5 ± 13.6 and 608.6 ± 16.2 mg N L^{-1} in stages A, B and C, respectively) (Fig. 3). Although N was added to the pond in form of ammoniacal species, no N-NH_4^+ was detected in the cultivation broth as a result of an active nitrification to NO_2^- /NO_3^- and NH_4^+ uptake by microorganisms. In fact, despite the high pH in the cultivation broth, the nitrogen mass balance conducted indicated that only 18, 13 and 1% of the initial nitrogen and the total nitrogen input was lost via volatilization during stages A, B and C,

306 respectively (Table S1, Supplementary Material). Surprisingly, the predominant form of
307 dissolved nitrogen during stages A and B was $N\text{-}NO_2^-$ (average $N\text{-}NO_2^-$ concentrations of
308 389.2 ± 5.6 and 404.3 ± 35.0 mg N L^{-1}, and average $N\text{-}NO_3^-$ concentrations of 226.7 ± 11.0
309 and 133.1 ± 31.2 mg N L^{-1} under steady state in stages A and B, respectively) despite the DO
310 concentration in the pond remained always above saturation. This higher concentration of N-
311 NO_2^- compared to $N\text{-}NO_3^-$ could be explained by the higher growth rate of ammonia-
312 oxidizing bacteria (AOB) compared to nitrite-oxidizing bacteria (NOB) at temperatures over
313 27 ºC, photoinhibition of NOB due to excessive light irradiance, a potential NOB activity
314 inhibition due to high salinity and/or preferential $N\text{-}NO_3^-$ assimilation by microalgae as a
315 result of $N\text{-}NH_4^+$ depletion in the cultivation medium [38,40,41]. Interestingly, $N\text{-}NO_3^-$ was
316 the dominant specie of N during stage C despite the lower DO, with a final concentration of
317 540 mg N L^{-1} almost 10 folds higher than that of $N\text{-}NO_2^-$ (55 mg N L^{-1}) (Fig. 3). These
318 results could be attributed to the lower average irradiance in the cultivation medium due to a
319 mutual shading effect caused by the increase in both biomass concentration and residence
320 time, which likely enhanced NOB growth and nitrite oxidation [42]. This high nitrate
321 concentration could have contributed to microalgae inhibition during stage C since nitrate
322 uptake rate is typically lower than that of ammonia and high nitrate concentration in the
323 cultivation medium could cause an accumulation of intracellular nitrite [43].

324 <Fig. 3>

325 **3.2. Biogas upgrading**

326 During stage A, the CO_2 concentration in the upgraded biogas varied from 1.5 to 4.4%, which
327 corresponded to CO_2-REs between 96.6 and 89.5%, respectively. A more robust biogas
328 upgrading was obtained as a result of the increase in IC concentration in stage B, where CO_2
329 concentrations ranged from 0.6 to 0.8% (corresponding to CO_2-REs ranging between 98.4

330 and 98.1%). Similarly, CO_2 concentrations between 0.6 and 1.0% and CO_2-REs from 97.5 to
331 98.6% were recorded in stage C (Fig. 4a). These results were in agreement with Marín et al.
332 [21], who reported CO_2 concentrations fluctuating between 2.6 and 11.9% in the upgraded
333 biogas at IC concentrations of 1500-2000 mg C L^{-1}, which decreased to 0.7-2.1% at IC
334 concentrations > 2800 mg C L^{-1}. Similarly, Rodero et al. [44] observed a CO_2 concentration
335 increase from 2.7 to 12% due to the decrease in the pH of the cultivation medium from 9.50
336 to 9.05 at an IC concentration of ~1900 mg C L^{-1}. In this particular study, the increase in the
337 alkalinity of the cultivation medium from 1200 to 2400 mg IC L^{-1} supported stable CO_2
338 concentrations in the upgraded biogas and improved the robustness of the upgrading process.
339 These low CO_2 levels complied with the most restrictive values according to the recent
340 European standard EN 16723-1 for biogas injection into natural gas networks (≤ 2%) [4]. On
341 the other hand, the CO_2 values recorded during stage C gradually increased along with the
342 increase in the algal-bacterial biomass (Fig. 2 and 4). The high biomass concentrations
343 prevailing at the end of stage C could have negatively impacted on the CO_2 gas-liquid mass
344 transfer in the scrubbing biogas column as a result of biomass build-up on the diffuser.
345 However, this effect of the biomass concentration on CO_2 removal was no significant
346 ($p>0.05$, one-way ANOVA) due to the high IC concentration in the cultivation medium (up
347 to 3814 mg C L^{-1} by the end of stage C).
348
349 <Fig. 4>
350 On the other hand, H_2S-REs of 100% were achieved regardless of the alkalinity (1100-3800
351 mg IC L^{-1}) and the biomass concentration (0.3-1.38 g SSV L^{-1}) in the cultivation medium.
352 These higher eliminations compared to CO_2-REs were mediated by the higher aqueous
353 solubility of H_2S relative CO_2 according to their dimensionless Henry's law constants (C_L/C_G,

354 $H_{H2S} \approx 2.44$ *vs* $H_{CO2} \approx 0.83$ at 25 °C) and the rapid oxidation of H_2S in the liquid phase [45,46].
355 In this context, the high DO concentration and pH typically encountered in algal-bacterial
356 ponds lead to the formation of SO_4^{2-} as the major end-product of H_2S oxidation which can be
357 chemically supported by the DO concentration in the cultivation medium and/or biologically
358 by the action of aerobic sulfur-oxidizing bacteria, i.e. Thioalbus genus [44,47]. Similarly, a
359 complete H_2S removal was obtained regardless of the environmental conditions variations in
360 a similar system over one year operation using a high alkalinity digestate [21]. Franco-
361 Morgado et al. [15] also reported H_2S-REs of 99.5 ± 0.5% during biogas upgrading at IC
362 concentrations in the cultivation medium > 1000 mg C L^{-1}. These results confirmed the long-
363 term robustness of algal-bacterial processes under high-alkalinity conditions for H_2S
364 removal.
365
366 The low L/G ratio implemented in this study (0.5) constrained the amount of N_2 and O_2
367 stripped out from the recycling liquid to the biogas in the scrubbing column. In this regard,
368 average N_2 concentrations of 1.3 ± 0.4, 1.0 ± 0.3 and 0.8 ± 0.3%, and O_2 concentrations of
369 0.2 ± 0.1, 0.1 ± 0.1 and 0 ± 0.1% were recorded in the upgraded biogas during stage A, B
370 and C, respectively (Fig. 4c). Although a slight decrease in N_2 and O_2 desorption was
371 recorded during stages B and C, these differences were minimal. In fact, no-correlation
372 between the alkalinity and N_2 and O_2 stripping was obtained in a similar experimental set-up
373 at IC concentrations ranging from 100 to 1500 mg C L^{-1} at an L/G ratio of 0.5 [17]. The O_2
374 content in the upgraded biogas along the three stages was below the regulatory limits for
375 biomethane injection into natural gas networks or its use as vehicle fuel (≤ 1%) as a result of
376 the low L/G ratio set in this study.
377

Finally, CH_4 concentrations in the biomethane ranged from minimum values of 94.6, 97.8 and 98.0% to maximum values of 97.5, 98.9 and 98.7%, during stages A, B and C, respectively (Fig. 4b). Although, a good biomethane quality in terms of CH_4 concentration (≥ 95%) was achieved in the three operational stages, these values were more stable during stages B and C as a result of the consistent CO_2 removal and the low O_2 and N_2 stripping. In this context, the CH_4 concentrations achieved in this study were comparable to those recently reported in outdoors systems. Thus, Rodero et al. [44] recorded a CH_4 concentration of 97.3% in a similar configuration system at semi-industrial scale operating at a L/G ratio of 0.8, pH 9.5 and an IC concentration in the pond of ~1900 mg C L^{-1}, while Marín et al. [21] obtained a maximum CH_4 concentration of 97.8% in the upgraded biogas operating at a L/G ratio of 1, IC concentrations in the cultivation medium >2780 mg C L^{-1} and a pH of ~9.6.

3.3. Volumetric gas-liquid

3.4. Mass transfer coefficient and CO_2 stripping

The gas-liquid mass transfer performance of the open pond was evaluated under steady H_2S removal in stage B. The respirometric characterization performed in these days yielded average QO_2 and PO_2 values of 10.1 ± 3.0 and 11.3 ± 0.1 mg O_2 g SSV^{-1} h^{-1}, respectively. These QO_2 values were in agreement with previous studies reporting endogenous respiration rates of microalgae-bacteria cultures in the range of 4-6 mg O_2 g VSS h^{-1} [48,49]. Likewise, Sforza et al. [50] reported PO_2 values in the range of 6-15 mg O_2 g VSS h^{-1} for microalgae-bacteria systems. The H_2S elimination capacity supported by the system was 107 mg H_2S m_{liquid}^{-3} h^{-1}, corresponding to a R_{ex} value of 204 mg O_2 m_{liquid}^{-3} h^{-1}. The values of QO_2, PO_2 and R_{ex} experimentally determined were used in Equation 2 to estimate k_La_{O2} and then k_La_{CO2} (Equation 7). The fitting of Equation 2 to the experimental dissolved O_2 concentrations is

shown in Figure S1 (supplementary material). Correlation coefficients (R^2) ranging from 0.97 to 0.99 were obtained, which confirmed that the experimental data were adequately described by the model.

Considering the three mass transfer characterizations performed in the pond, average k_La_{O2} and k_La_{CO2} values of 1.18 ± 0.30 and 1.05 ± 0.27 h^{-1} were retrieved, respectively. The k_La_{O2} obtained in this study was in the range of that reported by Franco-Morgado et al. [15] (0.83 h^{-1}) in a 25 L pond with a depth of 14 cm and an internal recirculation velocity of 15 cm s^{-1}. Similarly, Ouargui et al. [51] reported a k_La_{O2} of 0.76±0.12 h^{-1} in a full-scale pond of 400 m long, 2.5 m uniform width and 0.5 m deep with a recirculation time of 79 min. In addition, Pham et al. [52] obtained k_La_{O2} values of 0.8-3.1 h^{-1} with a liquid recirculation velocity in the range of ~15-45 cm s^{-1} in a pond of 386 cm long × 40 cm wide × 15 cm deep. Based on the empirical IC concentration and pH value, the H_2CO_3 (dissolved CO_2) concentration was calculated considering the dissociation equilibria of the inorganic carbon (pKd_1 and pKd_2 of 6.35 and 10.33, respectively). CO_2 stripping was then estimated based on k_La_{CO2} and the dissolved CO_2 concentration in the pond under steady state in each operational stage. An average stripping rate of 0.43 ± 0.08, 0.94 ± 0.31 and 1.30 ± 0.09 g C-CO_2 m_{liquid}^{-3} h^{-1} was estimated during stages A, B and C, respectively, which showed that even at the high pH values recorded in the pond, CO_2 can be stripped out due to the high IC concentration. These values corresponded to 14.5, 24.1 and 33.4% of the IC input to the system (C-CO_2 absorbed from the biogas and IC added in the MSM) in stages A, B and C, respectively. In this context, Meier et al. [14] recorded higher IC losses to the atmosphere of 57% in an open-photobioreactor at a cultivation broth pH of ~7.3. Based on IC equilibrium, the CO_2 stripping potential increases exponentially as pH decreases. However, these results were higher than

426 the 5% reported by Toro-Huertas et al. [53] in an alkaline cultivation medium (IC
427 concentration of 1320±140 mg IC L^{-1}) in a high rate algal pond operated at a recirculation
428 velocity of ~ 15 cm s^{-1} and a pH values between 9.3 and 9.8.
429
430 **4. Conclusions**
431 The alkalinity in the cultivation medium impacted both on the efficiency of CO_2 removal in
432 the biogas scrubbing column and on CO_2 fixation by microalgae in the pond. IC
433 concentrations > 2400 mg C L^{-1} enhanced the effectiveness and robustness of the upgrading
434 process at the expenses of a decreasing photosynthetic activity due to oxidative stress of
435 microalgae. In addition, high alkalinities can mediate high CO_2 stripping even at high pH
436 values, thereby decreasing the environmental benefits of this green technology. Finally, an
437 increase in biomass concentration induced a slight decrease on the CO_2 gas-liquid mass
438 transfer in the biogas scrubbing column and lower biomass productivities in the pond.
439
440 **Acknowledgements**
441 This work was supported by the regional government of Castilla y León and the European
442 FEDER Programme (CLU 2017-09 and UIC 071). The support from DGAPA-UNAM
443 through the PAPIIT project IA100719 is also acknowledged.
444
445 **References**
446 [1] Ryckebosch E, Drouillon M, Vervaeren H. Techniques for transformation of biogas
447 to biomethane. Biomass and Bioenergy 2011;35:1633–45.
448 doi:10.1016/j.biombioe.2011.02.033.

[2] Yousef AM, El-maghlany WM, Eldrainy YA, Attia A. Upgrading biogas to biomethane and liquid CO_2 : A novel cryogenic process. Fuel 2019;251:611–28. doi:10.1016/j.fuel.2019.03.127.

[3] Global Bioenergy Statistics. WBA Global Bioenergy Statistics 2018. World Bioenergy Assoc 2018:43.

[4] Muñoz R, Meier L, Díaz I, Jeison D. A review on the state-of-the-art of physical / chemical and biological technologies for biogas upgrading. Rev Environ Sci Bio/Technology 2015:727–59. doi:10.1007/s11157-015-9379-1.

[5] UNE-EN 16723. Natural gas and biomethane for use in transport and biomethane for injection in the natural gas network. 2016.

[6] Kapoor R, Ghosh P, Kumar M, Vijay VK. Evaluation of biogas upgrading technologies and future perspectives: a review. Environmental Science and Pollution Research; 2019. doi:10.1007/s11356-019-04767-1.

[7] San-Valero P, Penya-roja JM, Javier Álvarez-Hornos F, Buitrón G, Gabaldón C, Quijano G. Fully aerobic bioscrubber for the desulfurization of H_2S-rich biogas. Fuel 2019;241:884–91. doi:10.1016/j.fuel.2018.12.098.

[8] European Biogas Association Statistical Report.http://european-biogas.eu/2017/12/14/eba-statistical-report-2017-published-soon/ 2018.

[9] Sarker S, Lamb JJ, Hjelme DR, Lien KM. Overview of recent progress towards in-situ biogas upgradation techniques. Fuel 2018;226:686–97. doi:10.1016/j.fuel.2018.04.021.

[10] Ángeles R, Marín D, Rodero M del R, Pascual C, González-Sanchez A, de Godos I, et al. Chapter 8 - Biogas treatment for H_2S, CO_2, and other contaminants removal. In: Soreanu G, Dumont É, editors. From Biofiltration to Promis. Options Gaseous

Fluxes Biotreat., Elsevier; 2020, p. 153–76. doi:10.1016/B978-0-12-819064-7.00008-X.

[11] Nagarajan D, Lee D-J, Chang J-S. Integration of anaerobic digestion and microalgal cultivation for digestate bioremediation and biogas upgrading. Bioresour Technol 2019;290:121804. doi:10.1016/j.biortech.2019.121804.

[12] Bahr M, Díaz I, Dominguez A, González Sánchez A, Muñoz R. Microalgal-Biotechnology As a Platform for an Integral Biogas Upgrading and Nutrient Removal from Anaerobic Effluents. Environ Sci & Technol 2013;48:573–81. doi:10.1021/es403596m.

[13] Sun S, Ge Z, Zhao Y, Hu C, Zhang H, Ping L. Performance of CO_2 concentrations on nutrient removal and biogas upgrading by integrating microalgal strains cultivation with activated sludge. Energy 2016;97:229–37. doi:10.1016/j.energy.2015.12.126.

[14] Meier L, Barros P, Torres A, Vilchez C, Jeison D. Photosynthetic biogas upgrading using microalgae: Effect of light/dark photoperiod. Renew Energy 2017;106:17–23. doi:10.1016/j.renene.2017.01.009.

[15] Franco-Morgado M, Alcántara C, Noyola A, Muñoz R, González-Sánchez A. A study of photosynthetic biogas upgrading based on a high rate algal pond under alkaline conditions: Influence of the illumination regime. Sci Total Environ 2017;592:419–25. doi:10.1016/j.scitotenv.2017.03.077.

[16] Yan C, Zhu L, Wang Y. Photosynthetic CO_2 uptake by microalgae for biogas upgrading and simultaneously biogas slurry decontamination by using of microalgae photobioreactor under various light wavelengths, light intensities, and photoperiods. Appl Energy 2016;178:9–18. doi:10.1016/j.apenergy.2016.06.012.

[17] Rodero M del R, Posadas E, Toledo-Cervantes A, Lebrero R, Muñoz R. Influence of alkalinity and temperature on photosynthetic biogas upgrading efficiency in high rate algal ponds. Algal Res 2018;33:284–90. doi:10.1016/j.algal.2018.06.001.

[18] Marín D, Carmona-martínez AA, Lebrero R, Muñoz R. Influence of the diffuser type and liquid-to-biogas ratio on biogas upgrading performance in an outdoor pilot scale high rate algal pond. Fuel 2020;275:117999. doi:10.1016/j.fuel.2020.117999.

[19] Serejo ML, Posadas E, Boncz MA, Blanco S, García-Encina P, Muñoz R. Influence of biogas flow rate on biomass composition during the optimization of biogas upgrading in microalgal-bacterial processes. Environ Sci Technol 2015;49:3228–36. doi:10.1021/es5056116.

[20] Franco-morgado M, Toledo-cervantes A, González-sánchez A, Lebrero R, Muñoz R. Integral (VOCs, CO_2, mercaptans and H_2S) photosynthetic biogas upgrading using innovative biogas and digestate supply strategies. Chem Eng J 2018;354:363–9. doi:10.1016/j.cej.2018.08.026.

[21] Marín D, Posadas E, Cano P, Pérez V, Blanco S, Lebrero R, et al. Seasonal variation of biogas upgrading coupled with digestate treatment in an outdoors pilot scale algal-bacterial photobioreactor. Bioresour Technol 2018;263:58–66. doi:10.1016/j.biortech.2018.04.117.

[22] Rodero M del R, Carvajal A, Castro V, Navia D, de Prada C, Lebrero R, et al. Development of a control strategy to cope with biogas flowrate variations during photosynthetic biogas upgrading. Biomass and Bioenergy 2019;131. doi:10.1016/j.biombioe.2019.105414.

[23] De Farias Silva CE, Gris B, Sforza E, La Rocca N, Bertucco A. Effects of Sodium Bicarbonate on Biomass and Carbohydrate Production in Synechococcus PCC 7002

521 2016;49:241–6. doi:10.3303/CET1649041.
522 [24] Li J, Li C, Lan CQ, Liao D. Effects of sodium bicarbonate on cell growth , lipid
523 accumulation , and morphology of Chlorella vulgaris. Microb Cell Fact 2018:1–10.
524 doi:10.1186/s12934-018-0953-4.
525 [25] He H, Chen Y, Li X, Cheng Y, Yang C, Zeng G. Influence of salinity on
526 microorganisms in activated sludge processes : A review. Int Biodeterior
527 Biodegradation 2017;119:520–7. doi:10.1016/j.ibiod.2016.10.007.
528 [26] Manjrekar ON. Hydrodynamics and Mass Transfer in Bubble Columns. Engineering
529 and Applied Science Theses & Dissertations, 2016.
530 [27] Pringsheim EW, Koch W. Maintenance of Cultures- Spirulina Medium Recipe-Vers.
531 10. 2008. Sammlung von Algenkulturen Göttingen Cult Collect Algae 2008:10–2.
532 [28] Toledo-Cervantes A, Madrid-Chirinos C, Cantera S, Lebrero R, Muñoz R. Influence
533 of the gas-liquid flow configuration in the absorption column on photosynthetic
534 biogas upgrading in algal-bacterial photobioreactors. Bioresour Technol
535 2017;225:336–42. doi:10.1016/j.biortech.2016.11.087.
536 [29] Estrada JM, Dudek A, Muñoz R, Quijano G. Fundamental study on gas-liquid mass
537 transfer in a biotrickling filter packed with polyurethane foam. J Chem Technol
538 Biotechnol 2014;89:1419–24. doi:10.1002/jctb.4226.
539 [30] Wilke CR, Chang P. Correlation of diffusion coefficients in dilute solutions. AIChE
540 J 1955;1:264–70. doi:10.1002/aic.690010222.
541 [31] Eaton, A. D., Clesceri, L. S., Rice, E. W., Greenberg, A. E., & Franson MAH.
542 APHA: standard methods for the examination of water and wastewater. Centen Ed
543 APHA, AWWA, WEF, Washington, DC 2005.
544 [32] Posadas E, Marín D, Blanco S, Lebrero R, Muñoz R. Simultaneous biogas upgrading

and centrate treatment in an outdoors pilot scale high rate algal pond. Bioresour Technol 2017;232:133–41. doi:10.1016/j.biortech.2017.01.071.

[33] Latifi A, Ruiz M, Zhang C. Oxidative stress in cyanobacteria. FEMS Microbiol Rev 2009;33:258–78. doi:10.1111/j.1574-6976.2008.00134.x.

[34] Roselet F, Vandamme D, Roselet M, Muylaert K, Abreu PC. Effects of pH , Salinity , Biomass Concentration , and Algal Organic Matter on Flocculant Efficiency of Synthetic Versus Natural Polymers for Harvesting Microalgae Biomass 2017:427–37. doi:10.1007/s12155-016-9806-3.

[35] Ananyev G, Gates C, Dismukes GC. The Oxygen quantum yield in diverse algae and cyanobacteria is controlled by partitioning of flux between linear and cyclic electron flow within photosystem II. Biochim Biophys Acta - Bioenerg 2016;1857:1380–91. doi:10.1016/j.bbabio.2016.04.056.

[36] Li S, Wang P, Zhang C, Zhou X, Yin Z, Hu T, et al. Influence of polystyrene microplastics on the growth, photosynthetic efficiency and aggregation of freshwater microalgae Chlamydomonas reinhardtii. Sci Total Environ 2020;714:136767. doi:10.1016/j.scitotenv.2020.136767.

[37] Gong H, Tang Y, Wang J, Wen X, Zhang L, Lu C. Characterization of photosystem II in salt-stressed cyanobacterial Spirulina platensis cells. Biochim Biophys Acta - Bioenerg 2008;1777:488–95. doi:10.1016/j.bbabio.2008.03.018.

[38] Metcalf, Eddy. Wastewater Engineering: Treatment and Reuse. Fifth Edit. New York: McGraw-Hill; 2014.

[39] González-Sánchez A, Revah S. The effect of chemical oxidation on the biological sulfide oxidation by an alkaliphilic sulfoxidizing bacterial consortium 2007;40:292–8. doi:10.1016/j.enzmictec.2006.04.017.

569 [40] Marazzi F, Bellucci M, Rossi S, Fornaroli R, Ficara E, Mezzanotte V. Outdoor pilot
570 trial integrating a sidestream microalgae process for the treatment of centrate under
571 non optimal climate conditions. Algal Res 2019;39:101430.
572 doi:10.1016/j.algal.2019.101430.
573 [41] Jeong D, Cho K, Lee CH, Lee S, Bae H. Effects of salinity on nitrification efficiency
574 and bacterial community structure in a nitrifying osmotic membrane bioreactor.
575 Process Biochem 2018;73:132–41. doi:10.1016/j.procbio.2018.08.008.
576 [42] González-Camejo J, Montero P, Aparicio S, Ruano M V, Borrás L, Seco A, et al.
577 Nitrite inhibition of microalgae induced by the competition between microalgae and
578 nitrifying bacteria. Water Res 2020;172. doi:10.1016/j.watres.2020.115499.
579 [43] Montero P, Aparicio S, Ruano M V, Borr L, Barat R. Nitrite inhibition of microalgae
580 induced by the competition between microalgae and nitrifying bacteria 2020;172.
581 doi:10.1016/j.watres.2020.115499.
582 [44] Rodero R, Carvajal A, Arbib Z, Lara E, Prada C De. Performance evaluation of a
583 control strategy for photosynthetic biogas upgrading in a semi-industrial scale
584 photobioreactor. Bioresour Technol 2020;307:123207.
585 doi:10.1016/j.biortech.2020.123207.
586 [45] Sander R. Compilation of Henry's Law Constants for Inorganic and Organic Species
587 of Potential importance in Environmental Chemistry 1999.
588 [46] Meier L, Stará D, Bartacek J, Jeison D. Removal of H_2S by a continuous microalgae-
589 based photosynthetic biogas upgrading process. Process Saf Environ Prot
590 2018;119:65–8. doi:10.1016/j.psep.2018.07.014.
591 [47] Toledo-Cervantes A, Serejo ML, Blanco S, Pérez R, Lebrero R, Muñoz R.
592 Photosynthetic biogas upgrading to bio-methane: Boosting nutrient recovery via

biomass productivity control. Algal Res 2016;17:46–52. doi:10.1016/j.algal.2016.04.017.

[48] Grobbelaar JU, Soeder CJ. Respiration losses in planktonic green algae cultivated in raceway ponds. J Plankton Res 1985;7:497–506. doi:10.1093/plankt/7.4.497.

[49] Sánchez-Zurano A, Gómez-Serrano C, Acién-Fernández FG, Fernández-Sevilla JM, Molina-Grima E. A novel photo-respirometry method to characterize consortia in microalgae-related wastewater treatment processes. Algal Res 2020;47:101858. doi:10.1016/j.algal.2020.101858.

[50] Sforza E, Pastore M, Spagni A, Bertucco A. Microalgae-bacteria gas exchange in wastewater: how mixotrophy may reduce the oxygen supply for bacteria. Environ Sci Pollut Res 2018;25:28004–14. doi:10.1007/s11356-018-2834-0.

[51] El Ouarghi H, Boumansour BE, Dufayt O, El Hamouri B, Vasel JL. Hydrodynamics and oxygen balance in a high-rate algal pond. Water Sci Technol 2000;42:349–56. doi:10.2166/wst.2000.0678.

[52] Pham LA, Laurent J, Bois P, Wanko A. Impacts of operational conditions on oxygen transfer rate , mixing characteristics and residence time distribution in a pilot scale high rate algal pond 2018:1782–91. doi:10.2166/wst.2018.461.

[53] Toro-Huertas EI, Franco-Morgado M, de los Cobos Vasconcelos D, González-Sánchez A. Photorespiration in an outdoor alkaline open-photobioreactor used for biogas upgrading. Sci Total Environ 2019;667:613–21. doi:10.1016/j.scitotenv.2019.02.374.

616

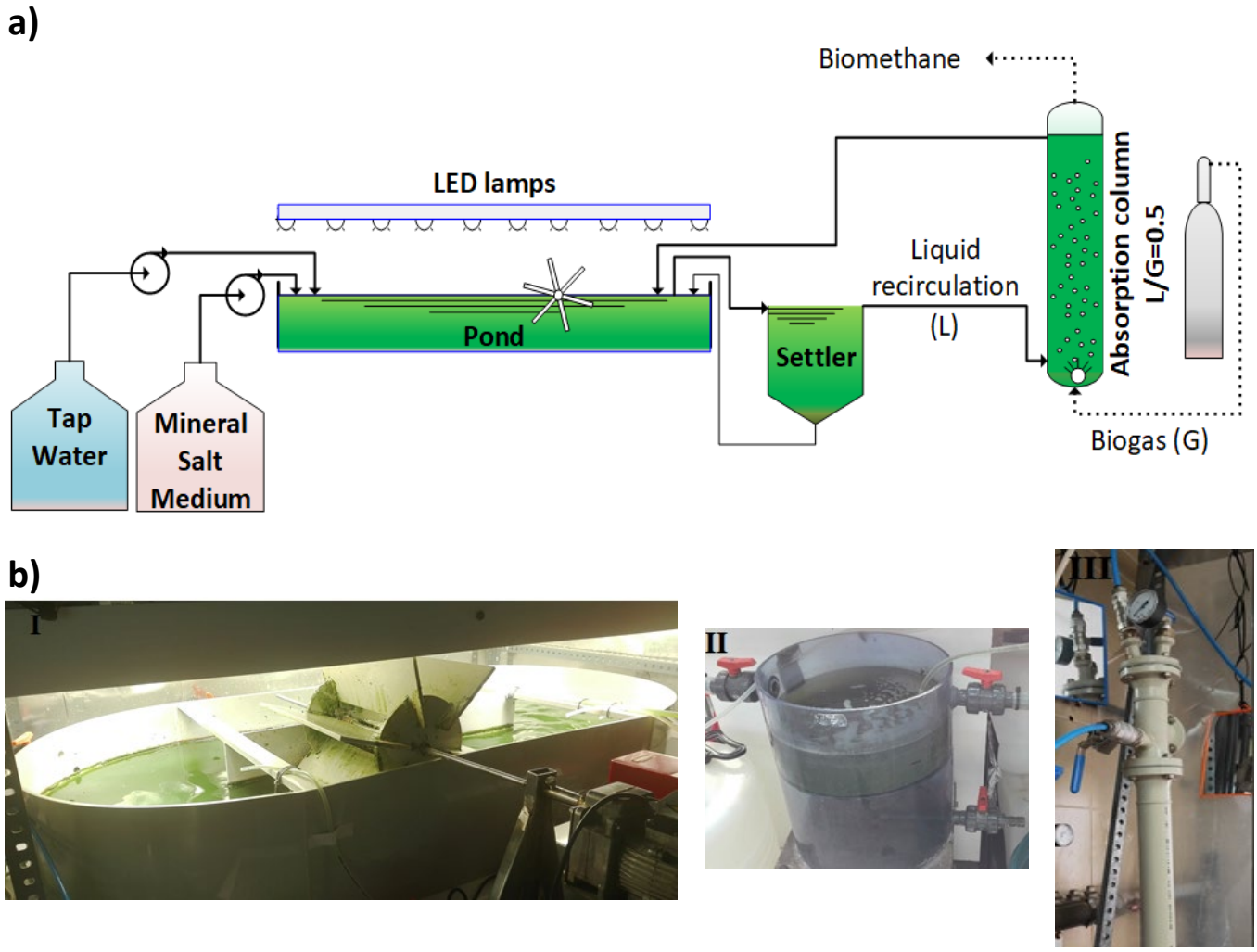

617 **Fig. 1.** a) Schematic diagram of the indoor experimental set-up for photosynthetic biogas
618 upgrading and b) photograph of the pilot scale system: I pond, II settler, III biogas scrubbing
619 column.

620

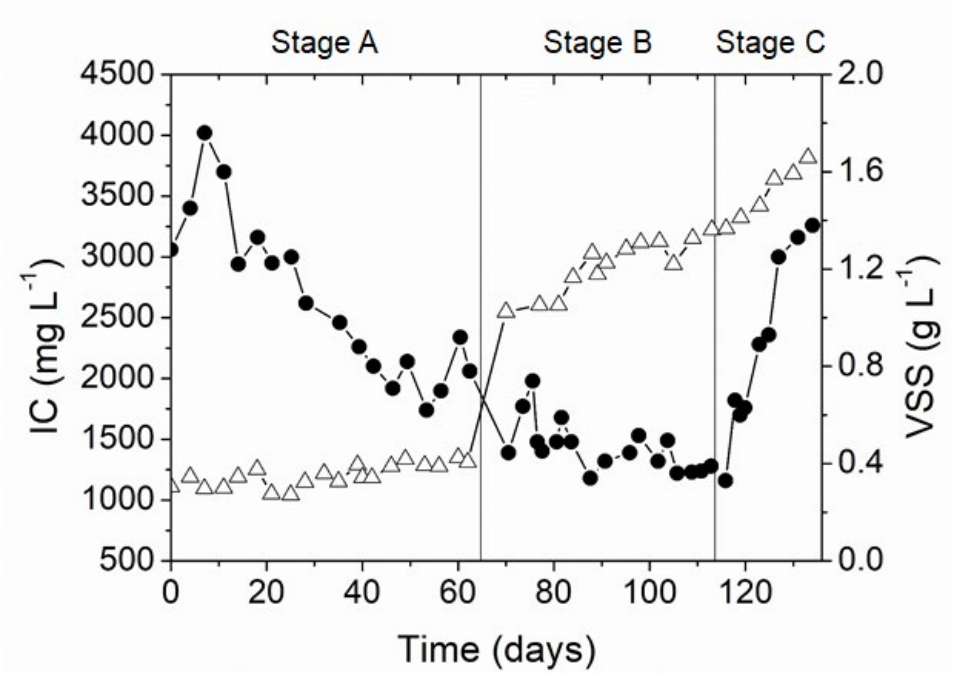

621

622

623 **Fig. 2.** Evolution of the concentration of inorganic carbon (IC, Δ) and volatile suspended

624 solids (VSS, ●) in the pond.

625

626

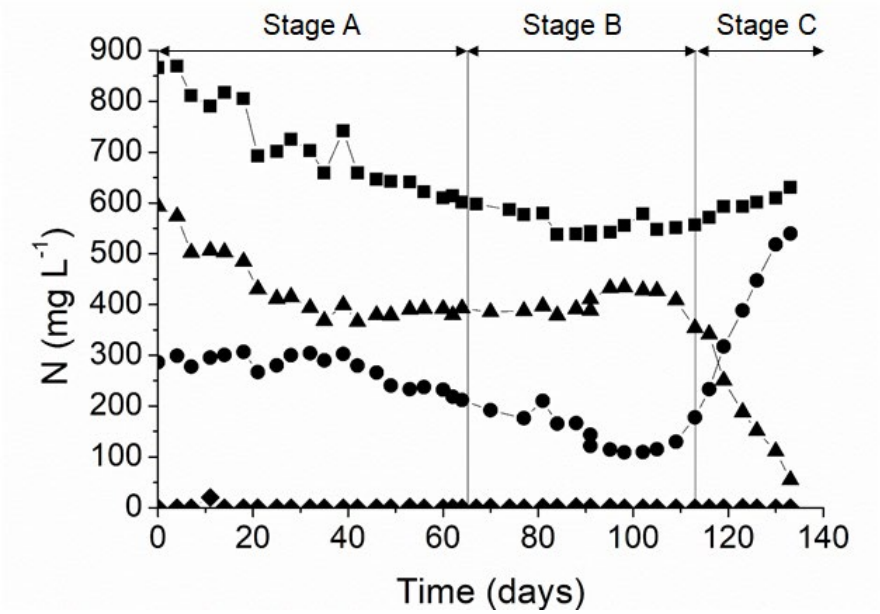

627

628 **Fig. 3.** Evolution of the concentration of nitrogen compounds in the pond: total nitrogen

629 (■), N-NH_4^+ (♦), NO_2^- (▲) and NO_3^- (●).

630

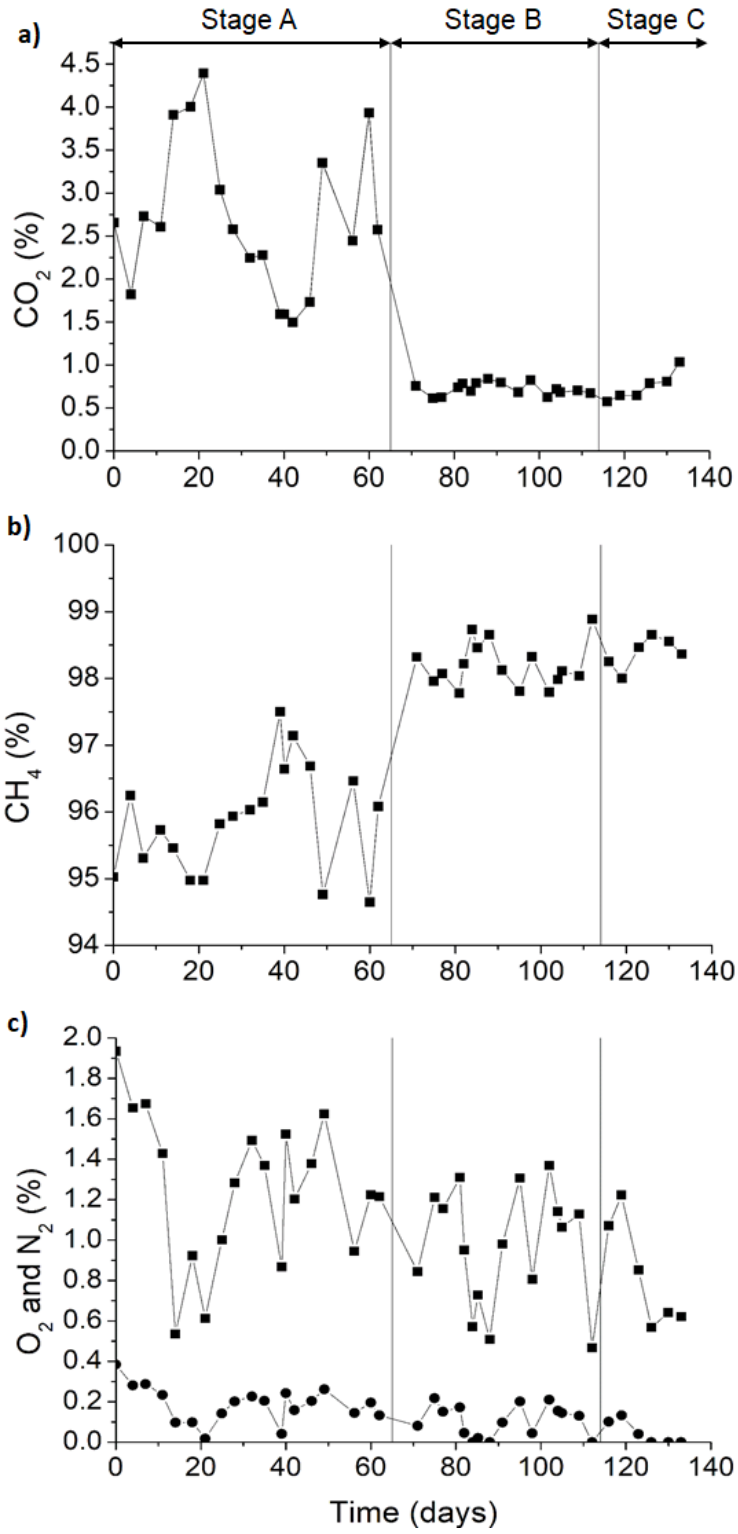

631

632 **Fig. 4.** Evolution of the concentration of a) CO_2, b) CH_4, c) O_2 (●) and N_2 (■) in the upgraded

633 biogas.

634

635 **Table 1.** Operational conditions applied during the three operational stages.

Stage	**A**	**B**	**C**
Period (days)	0-65	66-113	114-134
Inorganic carbon in the feed (mg L^{-1})	1200	2400	2400
Productivity (g m^{-2} d^{-1})	15	15	-

636

637 **Table 2.** Average environmental parameters (n=12) in the cultivation medium along with
638 their corresponding standard deviation under steady state conditions during the three
639 operational stages tested.

Stage	**A**	**B**	**C**
Cultivation broth temperature (ºC)	27.6 ± 0.6	29.5 ± 0.6	29.4 ± 0.6
DO (mg L^{-1})	12.8 ± 1.9	8.6 ± 0.9	4.4 ± 1.2
pH	9.7 ± 0.1	9.8 ± 0.1	9.7 ± 0
Evaporation rate (L m^{-2} d^{-1})	6.4±1.5	7.0 ± 0.6	6.8 ± 0.4

640